



Green synthesis of gold nanoparticles under sunlight irradiation and its colorimetric detection of Ni²⁺ and Co²⁺ ions

Journal:	<i>RSC Advances</i>
Manuscript ID:	RA-ART-11-2014-014034.R1
Article Type:	Paper
Date Submitted by the Author:	24-Dec-2014
Complete List of Authors:	M, Annadhasan; University of Madras, Department of Polymer Science J, Kasthuri; Quaid-E-Millath Government College for Women (Autonomous), Department of Chemistry Nagappan, Rajendiran; University of Madras, Polymer science

ARTICLE

Green synthesis of gold nanoparticles under sunlight irradiation and its colorimetric detection of Ni²⁺ and Co²⁺ ions

Cite this: DOI: 10.1039/x0xx00000x

M. Annadhasan^a, J. Kasthuri^b and N. Rajendiran^{a*}Received 00th January 2012,
Accepted 00th January 2012

DOI: 10.1039/x0xx00000x

www.rsc.org/

The present work describes the preparation of gold nanoparticles (AuNPs) under natural sunlight irradiation and its use in colorimetric detection of heavy metal ions. The AuNPs were prepared by an environmentally benign method using N-cholyl-L-valine (NaValC) as a self-reducing as well as stabilizing agent in aqueous medium. The size and shape of the particles were systematically controlled by varying the ratio of NaValC and Au³⁺ ions. The pH of the solution medium, sunlight irradiation and reaction time also influences the size and shape selectivity. The prepared NPs were thoroughly characterized by using UV-visible spectroscopy, TEM, DLS, EDX, XRD, XPS, FT-IR, Cyclic voltammetry and TGA techniques. Natural solar energy acting as a driving force for the generation of AuNPs in aqueous medium makes the process eco-friendly, attractive and economical. As these NPs are highly reactive towards surrounding environment the prepared AuNPs were effectively utilized for the colorimetric detection of Co²⁺ and Ni²⁺ ions in environmental samples.

Keywords: Gold nanoparticles, sunlight, green synthesis, N-cholyl-L-valine, colorimetric detection.

INTRODUCTION

In the ever-expanding field of nanomaterial research, gold nanoparticles (AuNPs) have attracted much interest over the last few decades due to its remarkable novel properties such as intense surface plasmon resonance (SPR) in the visible region, highly stable dispersions, chemical inertness and biocompatibility.^{1,2} A small change in the AuNPs size, shape, surface nature, and the distance between particles leads to tunable changes in their physical, chemical, optical and electronic properties of these nanoscopic materials,^{3,4} which find widespread applications in the field of fabrication of optical devices,⁵ catalysis,^{6,7} surface-enhanced Raman scattering (SERS),^{8,9} biological labeling,^{10,11} bio-imaging,^{12,13} drug delivery and antimicrobial agents,^{14,15} and so on. There are number of experimental recipes available in the literature for the preparation of AuNPs of variable size and shape through variety of synthetic approaches using numerous capping agents depending on their applications. Although these AuNPs synthesized by chemical and physical methods are biocompatible, however in some cases it involves toxic reducing agent, tedious and costly chemicals.¹⁶⁻¹⁸ The drawback of using additional reducing agents may complicate the recovery of the final products and also render them unsuitable for further biological or chemical applications. The other approaches quoted in the literature require high temperature and pressure or sophisticated techniques for the synthesis of NPs.

Hence, researchers were inspired to integrate “green chemistry” principles for designing environmentally benign materials and sustainable methods for minimizing chemical hazards to human health and the environment, reducing waste, and preventing pollution. To eliminate the use of toxic reducing agents, researchers begin to use carbohydrates,¹⁹ amino acids,^{20,21} vitamins,²² proteins,²³ biopolymers,²⁴ and other eco-friendly biological agents in the synthesis of AuNPs have been reported. *Wallen et al.*, demonstrated a green synthesis of AuNPs and Ag-Au bimetallic NPs using glucose and starch as reducing and stabilizing agents under heating condition.^{25,26} *Varma et al.*, group concentrated mostly on green synthesis of noble metal NPs using plant extracts, vitamins, bio-surfactants, and microwave irradiation.²⁷⁻³⁰ Plant tannin has been used as reductant and stabilizer for synthesis of Au-Pd core shell NPs.³¹ AuNPs has been synthesized using starch-glucose for electrochemical applications.³² There are many reports available for the synthesis of AuNPs using plant extracts.³³⁻³⁶

Synthesis of metal NPs using sunlight and stabilizing them by biocompatible capping agents provide great advancement over existing chemical and physical methods, as solar energy is considered to be the largest source of carbon neutral renewable energy, cost-effective, eco-friendly and traceless in chemical processes. *Yeh et al.*,³⁷ reported on the synthesis of gold nano-decahedra using sunlight irradiation for ultrasensitive lead-ion

detection. *Luo*, demonstrated the size controlled synthesis of AuNPs using polyelectrolyte under sunlight irradiation.³⁸ *Liu and co-workers* synthesized bimetallic Ag-Au NPs using DNA template for sensing of TNT and tumor.³⁹ Size controlled AuNPs were synthesized using citrate as stabilizing agent under sun light irradiation.⁴⁰ *Ozaki and his co-workers* demonstrated the synthesis of Au nanoplates under sunlight irradiation using starch as reducing and stabilizing agents.⁴¹ Dissolved organic matters have been utilized for the synthesis of AgNPs and AuNPs under sunlight irradiation.⁴² Earlier, our research group reported the synthesis of AgNPs under sunlight irradiation using amino acid conjugated bile acid as stabilizing agent.⁴³ More recently, we reported a rapid synthesis of AgNPs and AuNPs using amino acid as both reducing and capping agent under sunlight irradiation for colorimetric detection of Pb^{2+} , Hg^{2+} and Mn^{2+} ions.⁴⁴

Heavy metals are reported to be possible environmental pollutants as many of them are toxic even at trace (ppm) level concentrations. Therefore, determination of toxic metals in the biological system and aquatic environment has become a vital need for remedial processes. In recent years, AgNPs and AuNPs have been extensively used for colorimetric detection of heavy metal ions due to their tunable size and distance-dependent optical properties with high extinction coefficients at the visible region.⁴⁵⁻⁴⁸ However, only few reports are available for detection of Co^{2+} and Ni^{2+} ions using NPs as colorimetric probe. Detection of these ions is important because of its widespread occurrence in ambient air, water, soil, food, animals, and plants. Cobalt is an essential element for nutrition and whose deficiency may cause anaemia, retarded growth and loss of appetite. Cobalt ions are the component of vitamin B-12, which is required for good health.⁴⁹ Consumption of cobalt in large doses may cause effects in lung, which include respiratory irritation, coughing, asthma, pulmonary edema and pneumonia.⁵⁰ Similarly nickel (Ni^{2+}) is an essential element, which involves in various enzyme activities such as hydrogenases, acetyl-coenzyme, carbon monoxide dehydrogenases, and catalytic processes.⁵¹ However consumption of nickel in excess may lead to adverse health effects like dermatitis, allergy, carcinogenesis and even cell death.⁵² For example, bifunctionalized AgNPs was used for colorimetric detection of Co^{2+} ions by *Li et al.*⁵³ *Jain and co-workers* have reported colorimetric and fluorometric detection of Co^{2+} ions using calix [4] pyrrole octa-hydrazide capped AuNPs in aqueous medium.⁵⁴ *Han et al.*, reported the colorimetric detection of Ni^{2+} ions using glutathione stabilized AgNPs.⁵⁵ *Graham et al.*, demonstrated the trace level detection of Ni^{2+} ions using functional AuNPs.⁵⁶ Hence in this present investigation we report a sunlight induced green synthesis of AuNPs using NaValC as capping and reducing agent under sunlight irradiation. These AuNPs were used for colorimetric detection of Co^{2+} and Ni^{2+} ions at nM concentrations in aqueous medium. This method ascertains to be an effective practical applicability in analysis of real water system (tap water and drinking water) from the surrounding area.

EXPERIMENTAL

Materials

Hydrogen tetrachloroaurate trihydrate ($\text{HAuCl}_4 \cdot 3\text{H}_2\text{O}$), potassium nitrate (KNO_3), potassium bromide (KBr), cholic acid (CA), L-valine (Val), were obtained from Sigma-Aldrich. *N*-cholyll-L-valine (CVal) was prepared according to our previous report.⁴³ Salts of the different cations for the study [BaCl_2 , CaCl_2 , CdCl_2 , CoCl_2 , $\text{Cr}(\text{NO}_3)_3$, CuCl_2 , FeSO_4 , HgCl_2 , NaCl , MgCl_2 , MnSO_4 , NiCl_2 , $\text{Pb}(\text{NO}_3)_2$ and ZnCl_2] were procured from SRL chemicals Pvt. Ltd. (India). All the heavy metal salt solutions (1×10^{-5} M) used for the experiments were prepared by mixing the required amount of salt in triple distilled water. Sodium hydroxide (NaOH) and hydrochloric acid (HCl) was used for adjusting the pH of the medium. All glassware's were cleaned with aqua-regia (HNO_3 , HCl 1:3 ratio) then with triple distilled water prior to use.

Instruments

UV-visible spectra were recorded on Techcomp UV-2301 spectrophotometer containing double beam in an identical compartments each for reference and test solution fitted with 1 cm path length quartz cuvettes. The Fourier transform infrared (FT-IR) spectra were recorded Nicolet 5700 FT-IR with 1 cm^{-1} resolution, by using compressed films of KBr pellets and sample powders. High resolution transmission electron microscopic (HR-TEM) images were recorded with a JEOL JEM 2100 equipped with a Gatan imaging filter. X-ray photoelectron spectroscopy (XPS) measurements were performed with Omicron Nanotechnology, GmbH, Germany XM1000 monochromator with Al $\text{K}\alpha$ radiation of 1483 eV operated at 300 W (20 mA emission current, 15 kV) and a base pressure of 5×10^{-5} mbar. Dynamic light scattering (DLS) measurements were performed for colloidal solutions using Nanotracc Ultra NPA 253 from Microtrac, U.S.A. Cyclic voltammograms (CV) were recorded using a computer-controlled 400A electrochemical analyzer using conventional three electrode (glassy carbon (GC), Pt wire and Ag/AgCl). Powder X-ray diffraction (XRD) of all samples were recorded on SMART Bruker D8 Advance diffractometer using Cu $\text{K}\alpha$ X-radiation ($\lambda = 1.54056 \text{ \AA}$) at 40 kV and 30 mA. Diffraction patterns were collected over a 2θ range of $5-80^\circ$ at a scan rate of 1° min^{-1} . Thermo gravimetric analysis (TGA) were carried out on (Netzsch STA 409PC) TG-DTA instrument from $30-800^\circ\text{C}$ with a scanning rate of $10^\circ\text{C}/\text{minute}$ in presence of nitrogen flow.

Synthesis of AuNPs

Stock solutions of HAuCl_4 (1.0×10^{-3} M), and sodium salt of *N*-cholyll-L-valine (NaValC) (1.0×10^{-3} M) were prepared using triple-distilled water, and the subsequent dilutions were made from the stock solution. In order to optimize the reaction condition, 0.3 mL of $\text{HAuCl}_4 \cdot 3\text{H}_2\text{O}$ solution was added into different concentrations of NaValC solution (1.6×10^{-5} M to 3.3×10^{-4} M), and the final volume was adjusted to 3.0 mL

using triple distilled water at basic pH. The reaction mixture was then shaken well and kept under bright sunlight. The formation of AuNPs was observed by the gradual change in solution color from light yellow to colorless and finally to red depending on the concentration of NaValC used in the reaction mixture. The reaction was completed within 20 minutes and the results were monitored by UV–visible spectrophotometer. After completion of the reaction, the synthesized NPs was centrifuged, and redispersed in water. The dispersion and centrifugation process was repeated thrice to remove any unreacted Au^{3+} ions or NaValC from the final product. The synthesized AuNPs further characterized and used for colorimetric sensing of heavy metal ions.

Colorimetric assay

An aliquot of 2 mL of NaValC–AuNPs was taken in a transparent glass vials, then known concentration of heavy metal ions were placed in all vials. Subsequently, the responses were recorded after 5 minutes of incubation using UV-visible spectroscopy. The experiments were carried out under identical conditions to optimize the detection limit. All experiments were repeated three times for the concordant responses. For the real water analysis, tap water and drinking water samples were collected in the nearby area and filtered prior to use.

RESULTS AND DISCUSSIONS

The effect of NaValC composition on the formation of AuNPs

The formation of AuNPs was monitored by UV-visible spectroscopy by measuring the intensity of SPR band in the wavelength range between 400 and 900 nm. The reaction was demonstrated by addition of 0.3 ml of (1.0×10^{-3} M) HAuCl_4 ions to various concentrations of NaValC ranging from 1.6×10^{-5} M to 3.3×10^{-4} M in aqueous medium under ambient sunlight irradiations as shown in Fig. 1. At low concentrations of NaValC capped AuNPs showed a broad SPR peak around 550nm with minimum intensity however, the intensity of SPR band steadily increases with blue shift (λ_{max} 520 nm) upon increase in the concentration of NaValC up to 3.3×10^{-4} M. After that there is no significant change in the intensity of SPR band was noted, indicating the completion of the reaction. Accordingly, the colorless solution gradually changed to intense pink depending upon the concentration of NaValC used in the reaction mixture. The variation seen in the intensity of the peak position with respect to substrate concentration may be due to existence of different size/shape of the NPs which was further confirmed by TEM and DLS analysis.

Effect of pH variation on the AuNPs formation

The NaValC containing three functional groups such as hydroxyl ($-\text{OH}$), imine ($-\text{NH}$) and carboxylate ($-\text{COO}^-$) were sensitive to pH variations and act as active sites for the reduction of metal salts and stabilization of NPs respectively. Therefore, the effect of pH on the synthesis of NaValC capped AuNPs was studied at different pH ranging from 6.0 to 12.0,

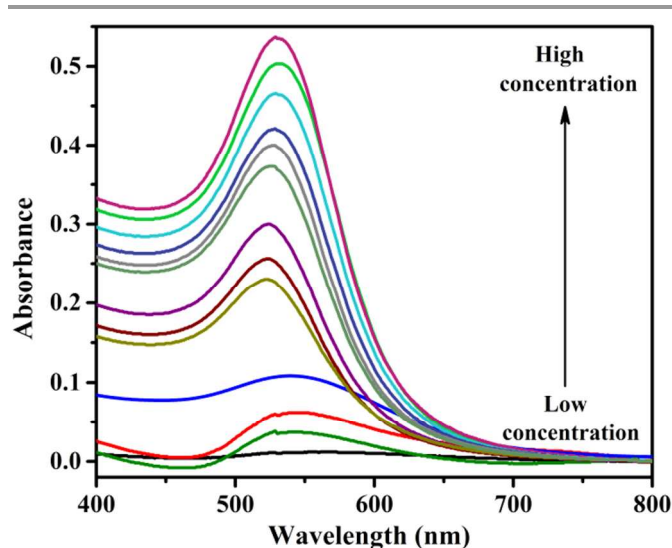


Fig.1. UV-vis spectra of the AuNPs prepared by various concentrations of NaValC ranging from 1.6×10^{-5} to 3.3×10^{-4} M.

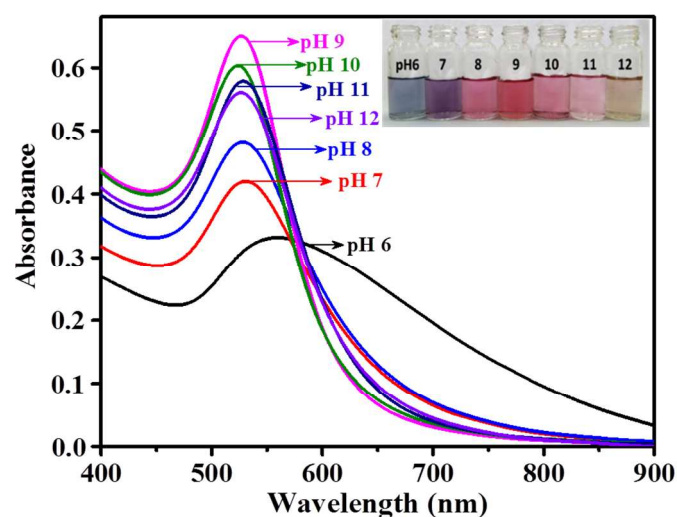


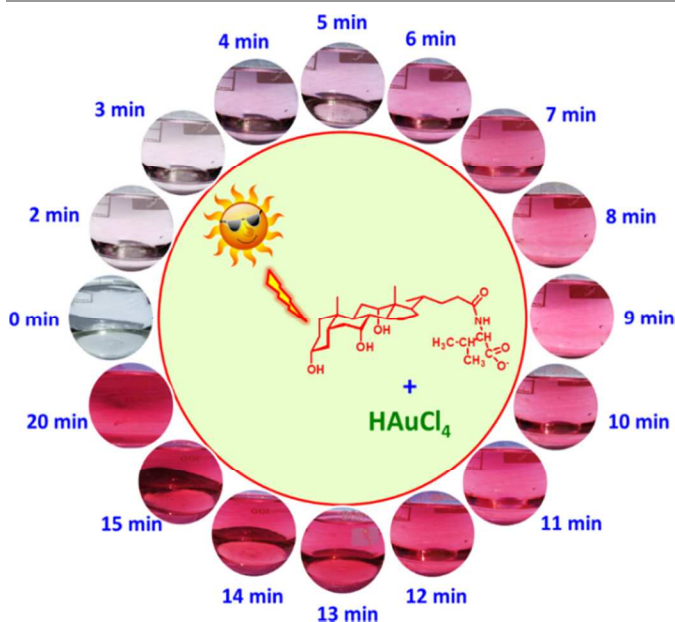
Fig.2. UV-visible spectra of NaValC stabilized AuNPs synthesized under sunlight irradiation at different pH ranging from 6-12. Inset shows the photograph of the corresponding solutions.

under sunlight irradiation as shown in Fig. 2. At pH 6.0, the intensity of SPR band becomes very broad plateau and increased significantly with increase in pH from neutral to alkaline medium and showed maximum intensity at pH 9.0. With further increase in pH, the intensity of SPR band decreased remarkably due to the destabilization of metal NPs. In acidic pH, due to existence of higher proton concentration, the reducing capacity of functional groups decreases for the reduction of metal salts. However in basic pH, the reducing ability of these functional groups were enhanced, as the dissociation constant of these functional groups ($-\text{OH}$, $-\text{NH}$ and $-\text{COO}^-$) falls in the pH range between 8.0 and 11.0, and thus allowing the formation of more stable AuNPs. The variation seen in the peak intensity and width of the bands observed at different pH could be attributed to either of the formation of aggregates/anisotropic nanoparticles, accordingly

the colour of the solution changed from blue to light brown. Hence, pH 9.0 was chosen as the optimum pH for the stabilization of AuNPs.

Time dependent spectral evolution of AuNPs formation

In order to know the reaction completion period, the kinetics of the formation of AuNPs was monitored at various time intervals using optimized concentration of 1.0×10^{-4} M of HAuCl_4 with 1.0×10^{-3} M of NaValC at basic pH 9.0 under sunlight irradiation (Fig. 3). Initially, no characteristic SPR peak was observed. After 2 minutes, the spectra of the suspensions have a characteristic absorption maximum ~ 524 nm, which is attributed to the surface plasmon resonance (SPR) of the AuNPs. As the reaction proceeds, the intensity of the absorption band increased with time up to 20 min without any notable shift in the λ_{max} indicating the size selectivity of the AuNPs. Accordingly the colorless solution gradually changes from light yellow to purple within 5 min, and finally to a red colour at 20 min (Scheme-1). After that there was no significant change in the intensity of SPR band was noted when the irradiation time was extended up to 30 min, indicating that the reaction was completed. After 6 months of storage at RT, no significant change was observed in the peak position and intensity, showing that the synthesized NPs were more stable (see Fig. S1. ESI†). This could be due to NaValC act as effective template for the reduction and stabilization of AuNPs through hydrophilic and hydrophobic interactions. Present results were also compared with the results obtained by the conventional heating at 60°C , ambient conditions in the lab and UV light irradiation. All these observations suggest that sunlight has very strong influence on this reaction that leads to narrow peak with high intensity and the reaction was completed within 20 minutes (see Fig. S2 ESI†).



Scheme-1 Schematic illustration of AuNPs formation at different time intervals under natural sunlight irradiation.

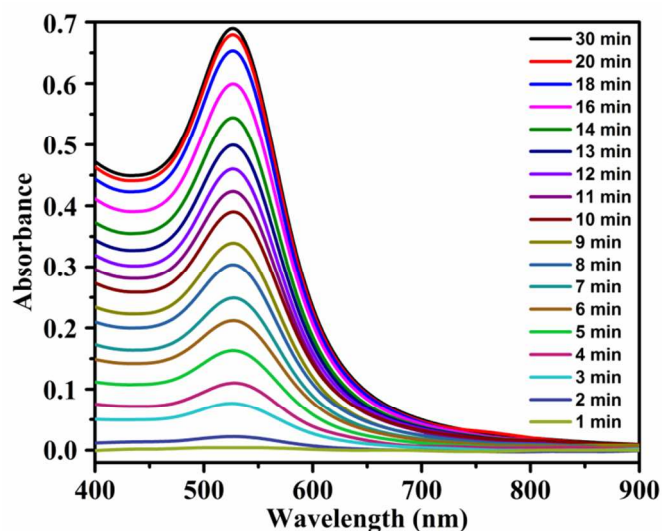


Fig. 3. UV-visible spectra of AuNPs formation at different time intervals under sunlight irradiation.

This could be due to the fact that when the mixture was exposed to sunlight, free radicals are generated owing to the decarboxylation of NaValC, subsequently the electron donating $\text{O}=\text{C}-\text{NH}$ and OH groups present in the capping ligand facilitate the charge transfer through photo induced electron transfer reaction for the reduction of Au^{3+} ions to $\text{Au}(0)$ state in the form of AuNPs. The above described processes get repeated and lead to the continuous growth of AuNPs and were stabilized by the capping agent through both hydrophobic and hydrophilic interactions.^{57,58} No AuNPs were formed without the addition of CVal even under sunlight irradiation.

TEM, XRD and DLS studies of AuNPs

Transmission electron microscopy, dynamic light scattering and X-ray diffraction studies have provided further insight into the morphology, size and crystallinity of the AuNPs. To observe the influence of the capping agent on the size and shape of the AuNPs, TEM image was recorded for low (1.0×10^{-4} M) and high (2.3×10^{-4} M) concentration of NaValC stabilized AuNPs at basic pH (Fig. 4 & 5). At low concentration of stabilizing agent the TEM images showed fused NPs along with few spherical shaped AuNPs with an average size of 40 nm, whereas at higher concentration well stabilized spherical shaped AuNPs were obtained with an average size of 8.0 nm. These results were consistent with DLS data (see Fig. S3. ESI †). This may be due to that at low concentration of capping agent, the reduction of metal ion is slow where the initially formed spherical nuclei become slow enough to fuse or join together to form fused AuNPs⁵⁹ (Fig 4a-d). However, at higher concentrations the formed particles are effectively stabilized by the stabilizing agent through hydrophobic and hydrophilic interaction that would have led to an enhanced nucleation rate with higher population of spherical shaped NPs. The selected area of electron diffraction (SAED) pattern obtained for AuNPs, clearly shows that the NPs were

crystalline in nature (Fig. 5e). The EDX analysis shows the composition of NaValC stabilized AuNPs (Fig. 5f).

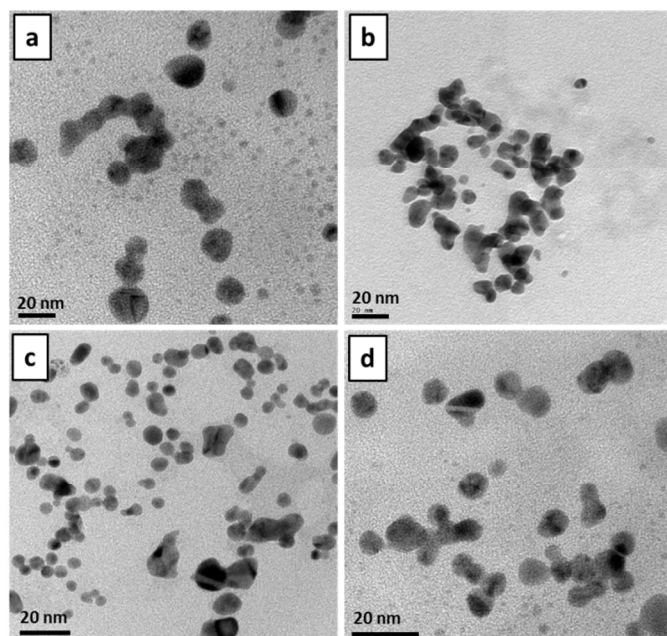


Fig. 4. TEM images of AuNPs stabilized using low concentration of NaValC 1.0×10^{-4} M with different magnifications (a–d).

The crystalline pattern of the prepared AuNPs was further confirmed by powder XRD analysis. The XRD pattern of the pure NaValC do not show any diffraction peak, but a broad hump was observed, which indicates the amorphous nature of the capping agent (Fig. 6). Bragg's reflections at $2\theta = 38.2$, 44.1 , 64.4 and 77.2 correspond to the $\{111\}$, $\{200\}$, $\{220\}$, and $\{311\}$ lattice planes respectively, for the fcc structure of AuNPs. The XRD pattern shows broad bands with strong intensity for the (111) and (200) reflections of the AuNPs, indicating that the size of the particles is in the nanometres range without any aggregation.

FT-IR and Cyclic voltammetry studies of AuNPs

The interactions of NaValC functional groups on the surface of metal NPs was demonstrated by mixing NaValC with HAuCl_4 solution under sunlight irradiation. The changes in the peak position were monitored by FT-IR spectroscopy at different time intervals and compared with pure NaValC as shown in Fig. 7. In the pure compound, the characteristic peak appeared at 1721 cm^{-1} and 1457 cm^{-1} corresponds to the asymmetric and symmetric stretching mode of $\text{O}-\text{C}=\text{O}$ group, 1650 cm^{-1} and 1544 cm^{-1} corresponds to the $\text{C}=\text{O}$ and $\text{HN}-\text{C}=\text{O}$ amide groups respectively. As the reaction proceeds, the characteristic peak for COO^- group has disappeared which could be attributed to the decarboxylation of NaValC under sunlight irradiation. The peaks for $\text{C}=\text{O}$ and $\text{HN}-\text{C}=\text{O}$ amide groups are merged together and exhibited as single peak at 1451 cm^{-1} after the completion of reaction, that shows the involvement of these functional groups in reduction and stabilization of NPs. Similar observation has been reported in the earlier studies.^{43,60}

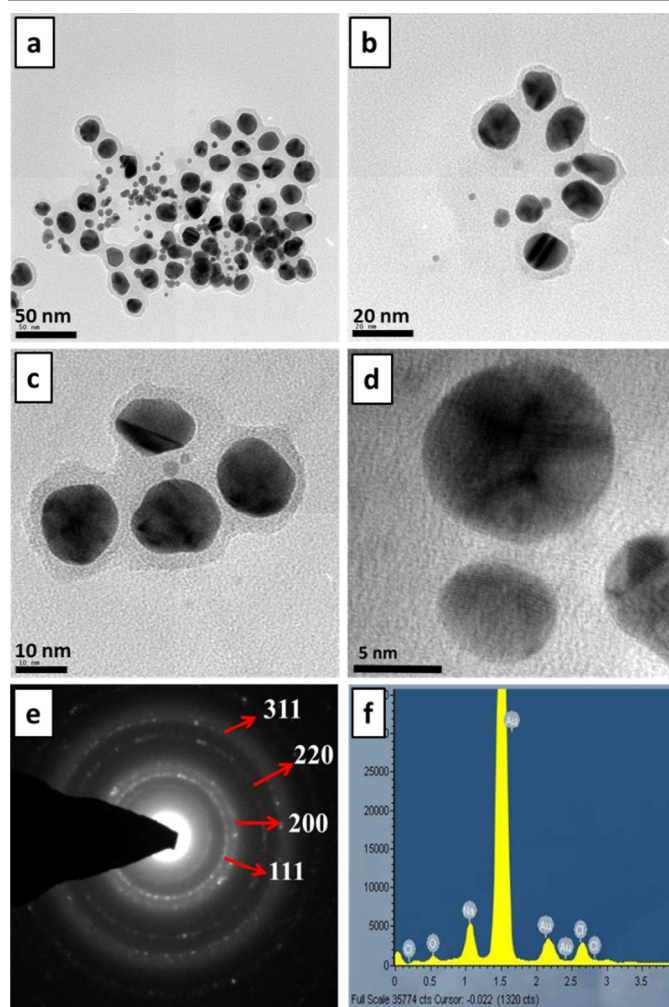


Fig. 5. TEM images of AuNPs stabilized with high concentration of NaValC 2.3×10^{-4} M (a–d) with different magnifications, and its corresponding (e) SAED pattern and (f) EDX.

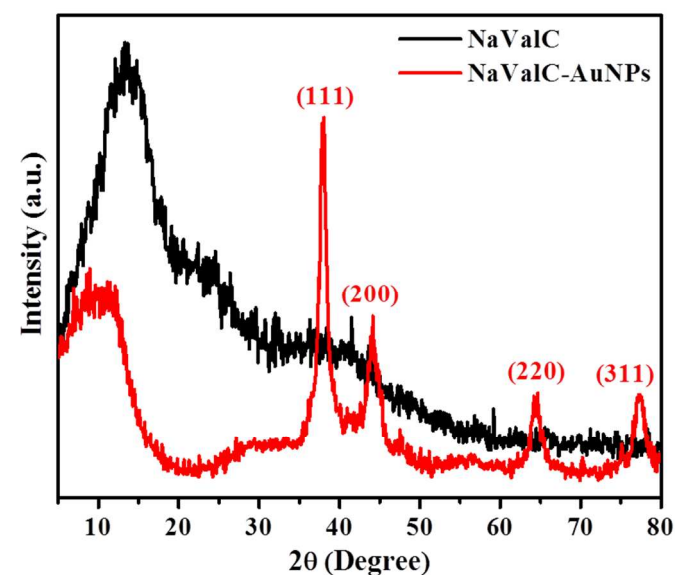


Fig. 6. Powder XRD pattern of pure NaValC and NaValC stabilized AuNPs.

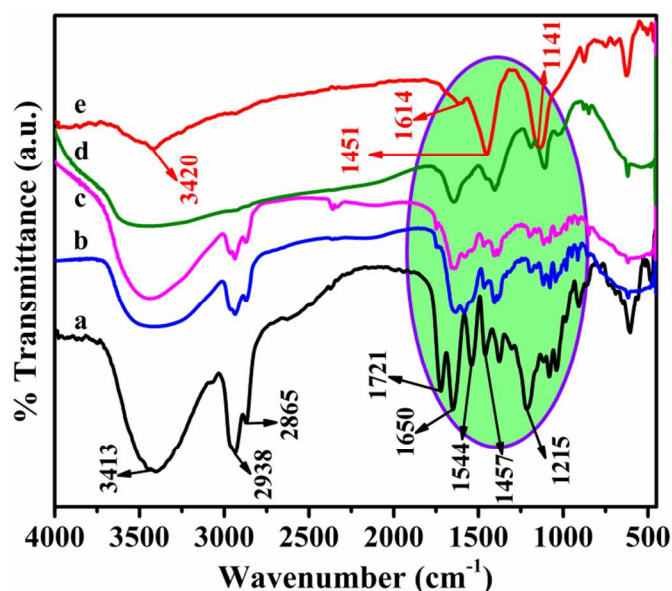


Fig. 7. FT-IR spectra of pure NaValC (a) and NaValC stabilized AuNPs at different time intervals under sunlight irradiation (b) 2 min, (c) 5 min, (d) 10 min and (e) 20 min.

Besides a peak appeared at 1215 cm^{-1} red shifted to 1141 cm^{-1} indicates the oxidation of OH group during the reduction of metal ions. Furthermore, the variation seen in the shape and peak position at 3413 cm^{-1} could be due to the contribution of -NH , and -OH groups for the reduction and stabilization of metal ions. The electrochemical behaviours of NaValC and NaValC capped AuNPs was studied by cyclic voltammetry technique using platinum electrode with fresh surface at scan rate of 25 mVs^{-1} . The inset of Fig. 8 curve shows the cyclic voltammograms of $1 \times 10^{-3}\text{ M}$ of HAuCl_4 ions in aqueous medium. The peak potential observed at 0.85 V corresponds to the stable irreversible reduction potential of HAuCl_4 ions.

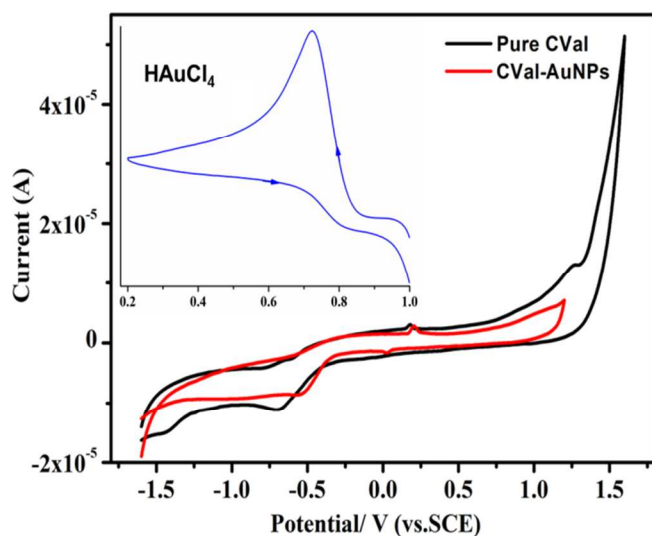


Fig. 8. Cyclic voltammetric response of pure NaValC with supporting electrolyte KNO_3 and NaValC stabilized AuNPs with KNO_3 . The inset shows $1.0 \times 10^{-3}\text{ M}$ HAuCl_4 response with KNO_3 ($1 \times 10^{-3}\text{ M}$) scan rate: 25 mV/s .

NaValC exhibited one reduction peak at -0.70 V and a small oxidation peak centered at $+1.25\text{ V}$ was observed in aqueous medium. After the reaction of NaValC with metal salts the redox peak potential of Au^{3+} ions completely vanishes, which clearly indicates the reduction of Au^{3+} ions to zero oxidation state in the form of AuNPs. This might be due to the electron donating -OH and amide group (-CONH-) groups of NaValC, which act as reducing functional groups on the NPs formation.

XPS studies of AuNPs

XPS measurements were performed to identify the elemental composition of the NaValC stabilized AuNPs. The survey spectrum of NaValC capped AuNPs showed the presence of Au 4f, C 1s, N 1s, and O 1s core levels (Fig. 9a). The Au 4f core-level curve fitted with two pairs of doublets from spin-orbital splitting of $4f_{7/2}$ (84.6) and $4f_{5/2}$ (88.2) (Fig. 9b). The position and difference between the two peaks (3.6 eV) almost exactly match the value reported for Au (0). The Au 4f peaks located at comparatively higher binding energy could be attributed to the binding of NaValC molecules on the surface of the AuNPs.

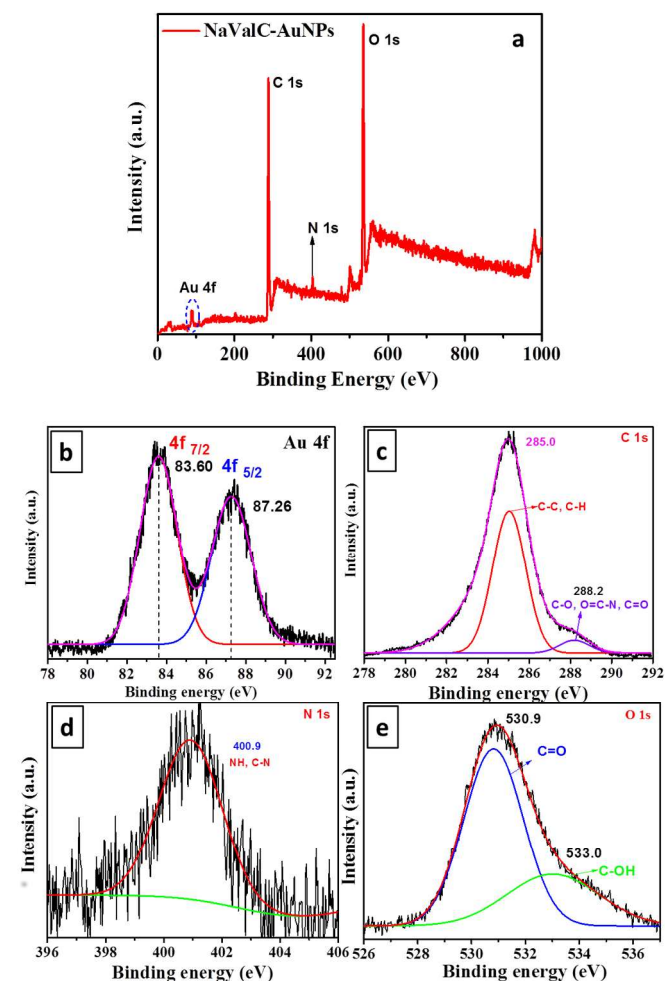


Fig. 9. XPS spectrum of NaValC stabilized AuNPs; survey spectrum (a), Au4f (b), C1s (c), N1s (d) and O1s (e).

The C 1s peak in Fig. 9c can be resolved into three main components namely, hydrocarbon (C–C, C–H), carbon bound to nitrogen i.e., amide and hydroxyl groups and (O=C–NH and C–OH) groups are located at 285.0 eV, and 288.2 eV respectively.⁶¹ The N 1s core level spectra (Fig. 9d) displays one symmetric peak centered at 400.9 eV and assigned to the nitrogen of the amide groups present in NaValC–AuNPs. The two peaks at 530.9 eV and 533.0 eV for the O 1s signal of NaValC, which is attributed to C=O in amide group and C–OH group respectively (Fig.9e). It reveals that these functional groups act as interaction sites for stabilization of metal NPs.

Thermo gravimetric analysis of NaValC–AuNPs

To investigate the thermal stability of NaValC capped AuNPs, TGA was recorded from carefully weighed powders of pure NaValC and NaValC stabilized AuNPs samples (Fig. 10). Two steps of thermal decomposition were observed for pure NaValC. The mass loss at the first step started around 120–310 °C which could be due to the decomposition of physically adsorbed water molecules and pyrolysis of the labile oxygen-containing carboxylate functional groups. However, in the second step a more rapid decomposition was observed around 310–450 °C and brought about a 70 wt% mass loss could be due to the decomposition of the remaining functional groups. Whereas in the case of NaValC stabilized AuNPs, the initial weight loss observed at 120 °C attributed to the physically adsorbed water molecules in the NaValC capped AuNPs and a small weight loss about 16% was observed from 310–450°C, due to decomposition of capping materials on the surface of the AuNPs. The improved thermal stability of NaValC capped AuNPs could be due to strong interaction of stabilizing agent on the surface of the AuNPs.

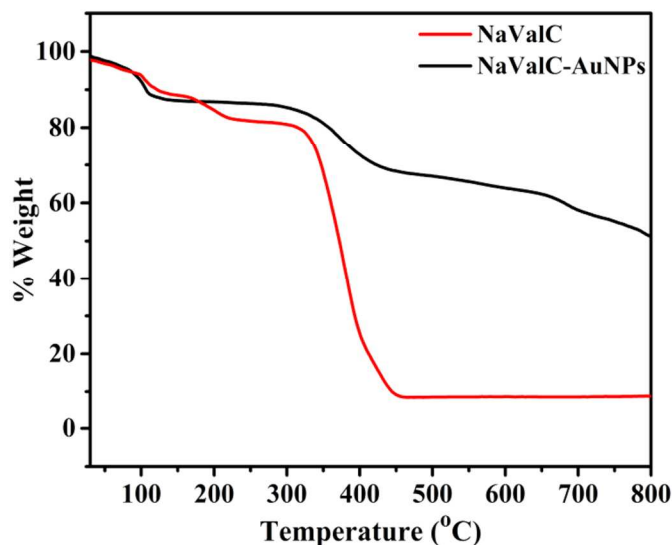


Fig.10. TGA curves of pure NaValC and NaValC stabilized AuNPs.

Colorimetric detection of heavy metal ions by NaValC–AuNPs

The optimized concentration of NaValC stabilized AuNPs was tested for their application as a colorimetric sensor because

of their size/shape dependent optical properties and tendency to agglomerate in the presence of analyte. To evaluate the sensitivity of AuNPs towards various metal ions, 200 nM concentration of metal ions were added to these NPs. Upon addition of various metal salts (Ba^{2+} , Ca^{2+} , Cd^{2+} , Cr^{3+} , Cu^{2+} , Fe^{2+} , Hg^{2+} , Mg^{2+} , Mn^{2+} , Na^+ , Pb^{2+} and Zn^{2+}) to the AuNPs solution, no visible color change was observed with any of these metal ions. However, a remarkable change in the intensity of the SPR band was observed when Ni^{2+} and Co^{2+} were added, and the color of the solution changed from pink to pale pink for Co^{2+} and violet for Ni^{2+} (Fig. 11a & b).

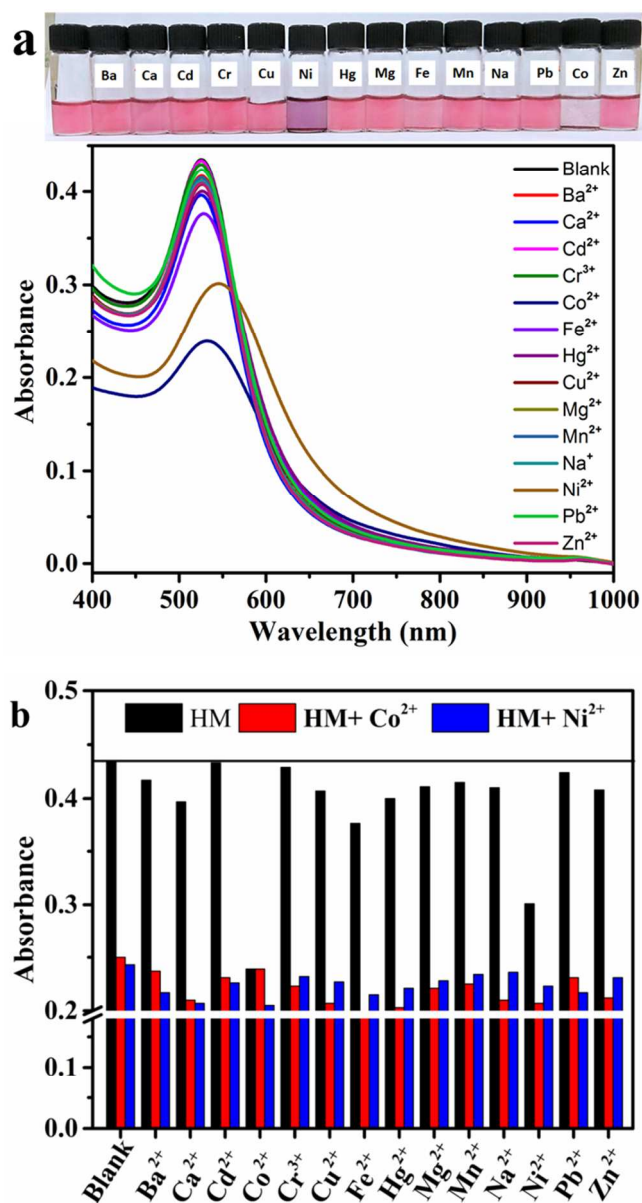


Fig.11. UV-visible spectra of AuNPs interaction with different metal ions (200 nM) and the photograph shows the color change (a). The black bars represent the addition of individual metal ions to the AuNPs solution while the red and blue bars shows the response of Co^{2+} and Ni^{2+} ions in the presence of other coexisting metal ions (b). HM - Heavy metal ions

Moreover, competitive experiments were also carried out by adding $\text{Ni}^{2+}/\text{Co}^{2+}$ ions to solutions of AuNPs in the presence of other cations. The coexistence of other cations shows significant spectral changes for AuNPs upon addition of $\text{Ni}^{2+}/\text{Co}^{2+}$ ions. These results indicate that the sensing of $\text{Ni}^{2+}/\text{Co}^{2+}$ ion possible in the presence of other metals.

Colorimetric detection of Ni^{2+} ions

Quantitative analysis was demonstrated by adding different concentrations of Ni^{2+} ions (0–100 nM) into the AuNPs solution and the changes in the intensity of SPR band was monitored by UV-visible spectroscopy. As shown in Fig. 12a, the intensity of SPR band gradually decreases along with shift towards longer wavelength from 524 nm to 543 as a function of Ni^{2+} concentration. In the presence of low concentration of Ni^{2+} ions the color of AuNPs changes from pink to purple, and then to violet in the presence of high concentration of Ni^{2+} . The color change of NPs solution could be due to the binding ability of functional groups on the NPs surface with Ni^{2+} through metal ligand interaction thereby the Ni^{2+} ions induced the aggregation of AuNPs.

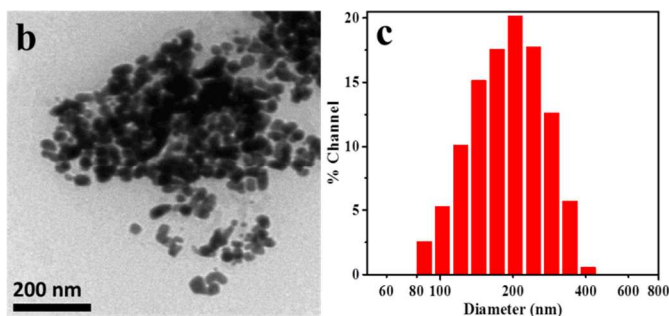
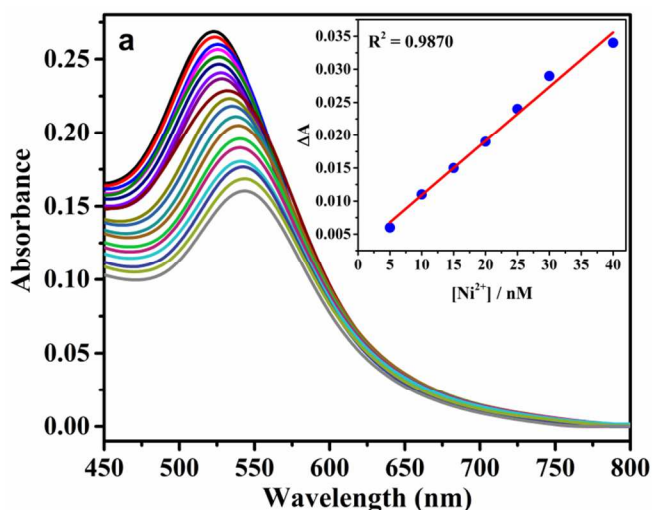


Fig. 12. UV-visible spectra of AuNPs after the addition of various concentrations of Ni^{2+} ions (0–100 nM) and the inset shows a linear plot of absorbance intensity difference versus concentration of Ni^{2+} ions (a). TEM images (b) and DLS histogram (c) of aggregated AuNPs after addition of 100 nM of Ni^{2+} ions.

A linear correlation of the differences in the absorbance intensity increased linearly with increasing the concentration of Ni^{2+} ranging from 5 nM to 40 nM and the value of linear

regression coefficient (R^2) was found to be 0.9870 with the lowest detection limit of 10 nM, making it suitable for the quantitative determination of Ni^{2+} ions at the nM level in aqueous solutions (Fig. 12a inset). Similar observation was reported by Han et al., by using glutathione protected AgNPs.⁵⁵ TEM and DLS studies were carried out in the presence and absence of Ni^{2+} ions, under identical conditions. A direct evidence for Ni^{2+} induced aggregation of the AuNPs was supported by TEM images and the increased hydrodynamic radius of the NPs from 12 nm to 193 nm was further confirmed by DLS analysis (Fig. 12 b & c). The difference in the TEM and DLS data are due to the fact that DLS measurements records higher values, since the light scattered from both core particle as well as layer on the surface of the NPs. Whereas in TEM measurement only the metallic particle core is measured. Further the zeta potential of AuNPs was found to be [−24.550 (mv)] and on addition of 100 nM Ni^{2+} ions, it was reduced to [+2.310 (mv)]. The significant change from negative to positive zeta potential indicates the formation of NPs aggregates through metal–ligand interaction between NaValC containing functional groups on the surface of the AuNPs with Ni^{2+} ions.

Colorimetric detection of Co^{2+} ions

Similarly, quantitative analysis was performed by adding different concentrations of Co^{2+} ions (0–100 nM) into the AuNPs solution and the changes in the intensity of SPR band were noted using UV-visible spectroscopy (Fig. 13). Upon addition of Co^{2+} ions into the AuNPs solution, the particles getting precipitation gradually and are deposited at the bottom of the ampule. Accordingly, the color of the solution faded pink to pale pink as a function of increase in concentration of Co^{2+} . This could be due to the higher affinities of functional groups present on the surface of the NPs with Co^{2+} ions through complexation. A linear correlation was observed with increasing the concentration of Co^{2+} ranging from 5 nM to 40 nM and the value of linear regression coefficient (R^2) was found to be 0.9806, with the lowest detection limit of 10 nM, making it suitable for the quantitative determination of Co^{2+} ions at nM level in aqueous solutions (Fig. 13 inset). In presence of Co^{2+} ions, the aggregation of NPs was confirmed by TEM analysis (Fig. 13) and the increase in the hydrodynamic radius of NPs from 12 nm to 176 nm was further supported by DLS studies. Further the zeta potential of AuNPs was found to be [−24.550 (mv)] and on addition of 100 nM Co^{2+} ions, it was reduced to [+4.790 (mv)]. The significant change from negative to positive zeta potential indicates the formation of NPs aggregation through metal–ligand interaction. We also conducted a competitive metal ion interaction for both metal ions (Ni^{2+} and Co^{2+}) with AuNPs under optimized conditions and the change in the optical absorbance was noted. The intensity of the SPR band decreases remarkably without any shift in the λ_{max} showing that Co^{2+} interact more effectively than the Ni^{2+} ion. The advantages of the present investigation over other methods are, it is simple, rapid, cost-effective sensing system with lower detection limit and very short response time (Table S1. ESI †).

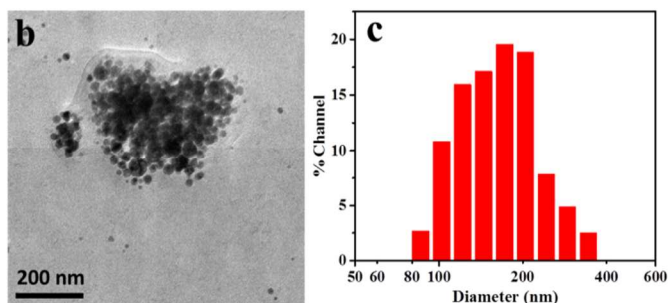
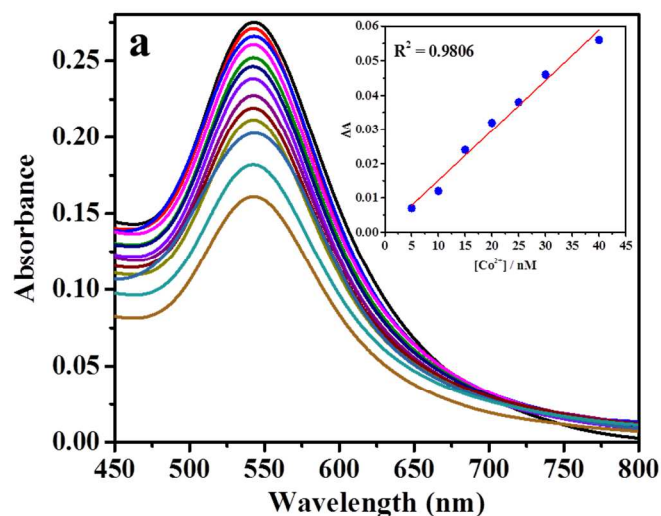


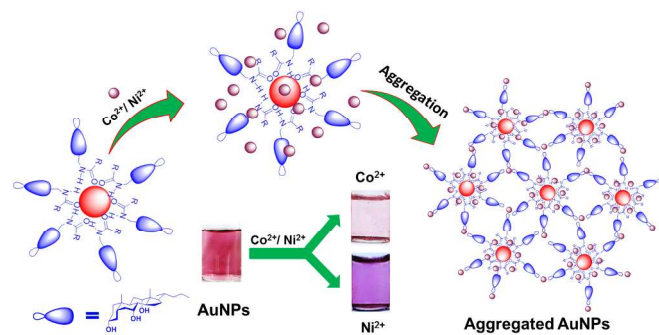
Fig. 13. UV-visible spectra of AuNPs after the addition of various concentrations of Co^{2+} ions (0–100 nM) and the inset shows a linear plot of absorbance intensity difference versus concentration of Co^{2+} ions. TEM images (b) and DLS histogram(c) of aggregated AuNPs after addition of 100 nM of Co^{2+} ions.

Based on the observed UV-visible spectral change, DLS studies, TEM images, and zeta potential measurements, we propose a possible mechanism for the interaction of AuNPs with $\text{Co}^{2+}/\text{Ni}^{2+}$ ions in aqueous medium as shown in Scheme-2. Upon addition of $\text{Co}^{2+}/\text{Ni}^{2+}$ into the AuNPs solution the intensity of SPR band gradually decreases with red shift for Ni^{2+} ions and without any shift for Co^{2+} ions. This could be due to the functional groups ($-\text{OH}$, $\text{C}=\text{O}$ and $\text{NH}-\text{C}=\text{O}$) present on the NPs surface complex with the metal ions ($\text{Co}^{2+}/\text{Ni}^{2+}$) through metal–ligand interactions. As a result these NPs closer to each other which led to the aggregation of NPs, accordingly the color of the solution changed from pink to violet for Ni^{2+} and pale pink for Co^{2+} .

Heavy metal detection in real water samples

The sensitivity and selectivity of AuNPs was tested in real samples such as tap water and drinking water. These samples were spiked with known concentration of metal ions (Ni^{2+} or Co^{2+}) and added to AuNPs. The responses for these real water samples were monitored by UV-visible spectroscopy. A linear decrease with a red shift in the absorption intensity was observed for Ni^{2+} ions in drinking and tap water, with the lowest detectable concentration of Ni^{2+} was estimated to be 15

nM and 10 nM in drinking water and tap water samples, respectively (see Fig. S4. ESI†).



Scheme-2. Schematic representation for the colorimetric recognition of Co^{2+} and Ni^{2+} ions using AuNPs in aqueous medium.

Similarly for Co^{2+} ions, also a linear decrease in the absorbance intensity was observed without any shift. The lowest detectable concentration of Co^{2+} was estimated to be 20 nM and 10 nM in drinking water and tap water samples, respectively (see Fig. S5. ESI†). The metal ion detection ability of the NaValC–AuNPs was significantly different when tested with real water samples (drinking water and tap water) in comparison to that of distilled and demineralized water. As in the real water samples more possibilities are there for dissolved organic and inorganic materials. These impurities have the chances to interact with the NPs and make them to aggregate much faster and hence the responses are quite better than pure water, i.e., deionized or demineralized water.

CONCLUSIONS

We have demonstrated an efficient, cost effective and eco-friendly approach for the synthesis of AuNPs in aqueous medium under sunlight irradiation. The size and shape of the NPs were tuned by varying the concentration of the NaValC, Au^{3+} ions, reaction time and pH of the medium. NaValC act as a self-reducing/stabilizing agent for the preparation of AuNPs and the reaction was completed within 20 minutes. The prepared AuNPs were characterized by UV-visible, TEM, DLS, EDX, XRD, XPS, FT-IR, Cyclic voltammetry and TGA techniques. The $-\text{OH}$ and $\text{NH}-\text{C}=\text{O}$ groups of NaValC were found to be involved in the reduction of the metal ions, while the hydrophobic and hydrophilic group stabilizes the NPs. The prepared AuNPs are highly stable in aqueous medium and do not show any signs of aggregation up to six months. The synthesized AuNPs were used as colorimetric sensors for selective detection Co^{2+} and Ni^{2+} ions over the other heavy metal ions in aqueous medium with detection limits of nM concentration. Also, this system is more suitable for rapid and convenient detection of Ni^{2+} and Co^{2+} ions in environmental water samples (tap water and drinking water) even with naked eyes. This method offers a new cost-effective, rapid, and simple procedure for potential applications in environmental water sample analysis.

Acknowledgements

The authors thank the Department of Science and Technology (NO SB/EMEQ-133/2013) (DST-EMEQ), Government of India, for their financial support. We also thank National Centre for Nanoscience and Nanotechnology (NCNSNT), University of Madras for HR-TEM studies and UGC-NRC, School of Chemistry, University of Hyderabad for powder XRD and TGA analysis.

Notes and references

^a Department of Polymer Science, University of Madras, Guindy campus, Chennai, Tamil Nadu, India-600 025.

^b Department of Chemistry, Quaid-E-Millath Government College for Women (Autonomous), Chennai, Tamil Nadu, India-600 002.

† Electronic Supplementary Information (ESI) available: [UV-visible spectrum, DLS analysis, Table and plots]. See DOI: 10.1039/b000000x/

- 1 L. M. Liz-Marzan, *Langmuir*, 2006, **22**, 32–41.
- 2 R. Shukla, V. Bansal, M. Chaudhary, A. Basu, R. R. Bhonde and M. Sastry, *Langmuir*, 2005, **21**, 10644–10654.
- 3 K. L. Kelly, E. Coronado, L. L. Zhao and G. C. Schatz, *J. Phys. Chem. B*, 2003, **107**, 668–677.
- 4 C. J. Murphy, T. K. San, A. M. Gole, C. J. Orendorff, J. X. Gao, L. Gou, S. E. Hunyadi and T. Li, *J. Phys. Chem. B*, 2005, **109**, 13857–13870.
- 5 C. Noguez and I. L. Garzón, *Chem. Soc. Rev.*, 2009, **38**, 757–771.
- 6 A. Corma and H. Garcia, *Chem. Soc. Rev.*, 2008, **37**, 2096–2126.
- 7 H. Yang, K. Nagai, T. Abe, H. Homma, T. Norimatsu and R. Ramaraj, *ACS Appl. Mater. Interfaces*, 2009, **1**, 1860–1864.
- 8 J. Yin, T. Wu, J. Song, Q. Zhang, S. Liu, R. Xu and H. Duan, *Chem. Mater.*, 2011, **23**, 4756–4764.
- 9 Y. Wang, B. Yan and L. Chen, *Chem. Rev.*, 2013, **113**, 1391–1428.
- 10 A. H. Jungemann, P. K. Harimech, T. Brown and A. G. Kanaras, *Nanoscale*, 2013, **5**, 9503–9510.
- 11 R. H. Menk, E. Schülte, C. Hall, F. Arfelli, A. Astolfo, L. Rigon, A. Round, K. Ataellmannan, S. R. MacDonald and B. H. Juurlink, *J. Nanomedicine*, 2011, **7**, 647–654.
- 12 C. L. Liu, H. T. Wu, Y. H. Hsiao, C. W. Lai, C. W. Shih, Y. K. Peng, K. C. Tang, H. W. Chang, Y. C. Chien, J. K. Hsiao, J. T. Cheng and P. T. Chou, *Angew. Chem. Int. Ed.*, 2011, **50**, 7056–7060.
- 13 L. Yang, L. Shang and G. U. Nienhaus, *Nanoscale*, 2013, **5**, 1537–1543.
- 14 G. Han, P. Ghosh and V. M. Rotello, *Nanomedicine*, 2007, **2**, 113–123.
- 15 Y. Zhang, H. Peng, W. Huang, Y. Zhou and D. J. Yan, *Colloid. Interf. Sci.* 2008, **325**, 371–376.
- 16 I. P. Santos and L. M. Liz-Marzan, *Langmuir*, 1999, **15**, 948–951.
- 17 S. Nath, S. Praharaj, S. Panigrahi, S. K. Ghosh, S. Kundu, S. Basu and T. Pal, *Langmuir*, 2005, **21**, 10405–10408.
- 18 Y. W. Tan, X. H. Dai, Y. F. Li and D. B. Zhu, *J. Mater. Chem.*, 2003, **13**, 1069–1075.
- 19 Z. Shervani and Y. Yamamoto, *Carbohydr. Res.*, 2011, **346**, 651–658.
- 20 P. R. Selvakannan, S. Mandal, S. Phadtare, R. Pasricha and M. Sastry, *Langmuir*, 2003, **19**, 3545–3549.
- 21 Y. Shao, Y. Jin and S. Dong, *Chem. Commun.*, 2004, **9**, 1104–1105.
- 22 P. Vemula, U. Aslam, V. A. Mallia and G. John, *Chem. Mater.*, 2007, **19**, 138–140.
- 23 S. L. Eichmann and M. A. Bevan, *Langmuir*, 2010, **26**, 14409–14413.
- 24 A. Pal, K. Esumi and T. Pal, *J. Colloid. Interf. Sci.*, 2005, **288**, 396–401.
- 25 P. Raveendran, J. Fu and S. L. Wallen, *J. Am. Chem. Soc.*, 2003, **125**, 13940–13941.
- 26 P. Raveendran, J. Fu and S. L. Wallen, *Green Chem.*, 2006, **8**, 34–38.
- 27 M. N. Nadagouda, G. Hoag, J. Collins and R. S. Varma, *Cryst. Growth Des.*, 2009, **9**, 4979–4983.
- 28 M. N. Nadagouda and R. S. Varma, *Green Chem.*, 2006, **8**, 516–518.
- 29 M. N. Nadagouda and R. S. Varma, *Cryst. Growth Des.*, 2007, **7**, 2582–2587.
- 30 B. Baruwati, V. Polshettiwar and R. S. Varma, *Green Chem.*, 2009, **11**, 926–930.
- 31 X. Huang, H. Wu, S. Pu, W. Zhang, X. Liao and B. Shi, *Green Chem.*, 2011, **13**, 950–957.
- 32 C. Engelbrekt, K. H. Sørensen, J. Zhang, A. C. Welinder, P. S. Jensen and J. Ulstrup, *J. Mater. Chem.*, 2009, **19**, 7839–7847.
- 33 S. K. Das, C. Dickinson, F. Lafir, D. F. Brougham and E. Marsili, *Green Chem.*, 2012, **14**, 1322–1334.
- 34 J. Kasthuri, S. Veerapandian and N. Rajendiran, *Colloids Surf. B*, 2009, **68**, 55–60.
- 35 S. Iravani, *Green Chem.*, 2011, **13**, 2638–2650.
- 36 R. K. Sharma, S. Gulati and S. Mehta, *J. Chem. Educ.*, 2012, **89**, 1316–1318.
- 37 Y. H. Chien, C. C. Huang, S. W. Wang and C. S. Yeh, *Green Chem.*, 2011, **13**, 1162–1166.
- 38 Y. Luo, *Mater. Lett.*, 2007, **61**, 2164–2166.
- 39 L. B. Yang, G. Chen, J. Wang, T. T. Wang, M. Li and J. Liu, *J. Mater. Chem.*, 2009, **19**, 6849–6856.
- 40 Y. Luo and X. Sun, *J. Nanosci. Nanotechnol.*, 2007, **7**, 708–711.
- 41 P. Pienpinijtham, X. X. Han, T. Suzuki, C. Thammacharoen, S. Ekgasit and Y. Ozaki, *Phys. Chem. Chem. Phys.*, 2012, **14**, 9636–9641.
- 42 Y. Yin, J. Liu and G. Jiang, *ACS Nano*, 2012, **6**, 7910–7919.
- 43 M. Annadhasan, V. R. Sankar Babu, R. Naresh, K. Umamaheswari and N. Rajendiran, *Colloids Surf. B*, 2012, **96**, 14–21.
- 44 M. Annadhasan, T. Muthukumarasamyvel, V. R. Sankar Babu and N. Rajendiran, *ACS Sustainable Chem. Eng.*, 2014, **2**, 887–896.
- 45 G. Aragay, J. Pons and A. Merkoci, *Chem. Rev.*, 2011, **111**, 3433–3458.
- 46 P. C. Ray, *Chem. Rev.*, 2010, **110**, 5332–5365.
- 47 H. N. Kim, W. X. Ren, J. S. Kim and J. Yoon, *Chem. Soc. Rev.*, 2012, **41**, 3210–3244.
- 48 E. M. Nolan and S. J. Lippard, *Chem. Rev.*, 2008, **108**, 3443–3480.
- 49 A. I. Stoica, M. Peltea, G. E. Baiulescu and M. Ionic, *J. Pharmaceut. Biomed.*, 2004, **36**, 653–656.
- 50 D. G. Barceloux and D. Barceloux, *Clin. Toxicol.*, 1999, **37**, 201–216.
- 51 A. Sigel, H. Sigel and R. K. O. Sigel, *John Wiley & Sons*, 2007, Vol. **2**, 728pp.
- 52 S. B. Mulrooney and R. P. Hausinger, *FEMS Microbiol. Rev.*, 2003, **27**, 239–261.

Journal Name

- 53 Y. Yao, D. Tian and H. Li, *ACS Appl. Mater. Interfaces*, 2010, **2**, 684–690.
- 54 K. D. Bhatt, D. J. Vyas, B. A. Makwana, S. M. Darjee and V. K. Jain, *Spectrochim. Acta. A.*, 2014, **121**, 94–100.
- 55 H. Li, Z. Cui and C. Han, *Sensor Actuat. B-Chem.*, 2009, **143**, 87–92.
- 56 Z. Krpetic, L. Guerrini, I. A. Larmour, J. Reglinski, K. Faulds and D. Graham, *Small*, 2012, **8**, 707–714.
- 57 N. S. Sariciftci, L. Smilowitz, A. J. Heeger and F. Wudl, *Science*, 1992, **258**, 1474–1476.
- 58 D. I. Pattison, A. S. Rahmanto and M. Davies, *J. Photochem. Photobiol. Sci.*, 2012, **11**, 38–53.
- 59 E. Dinda, M. Biswas and T. K. Mandal, *J. Phys. Chem. C*, 2011, **115**, 18518–18530.
- 60 S. Yang, Y. Wang, Q. Wang, R. Zhang, B. Ding, *Colloids Surf. A*, 2007, **301**, 174–183.
- 61 C. J. May, H. E. Canavan, D. G. Castner, *Anal. Chem.* 2004, **76**, 1114–1122.